

III. Particle interactions with matter

- ❖ All particle detecting techniques are based on interactions of particles with different materials

Short-range interaction with nuclei

- ❖ Probability of a particle to interact (with a nucleus or another particle) is called *cross-section*.
 - ☉ Cross-sections are normally measured in *millibarns*: $1 \text{ mb} \equiv 10^{-31} \text{ m}^2$
 - ☉ Total cross-section of a reaction is sum over all possible processes

There are two main kinds of scattering processes:

- ☉ *elastic scattering*: only momenta of incident particles are changed, for example, $\pi^- p \rightarrow \pi^- p$
- ☉ *inelastic scattering*: final state particles differ from those in initial state, like in $\pi^- p \rightarrow K^0 \Lambda$

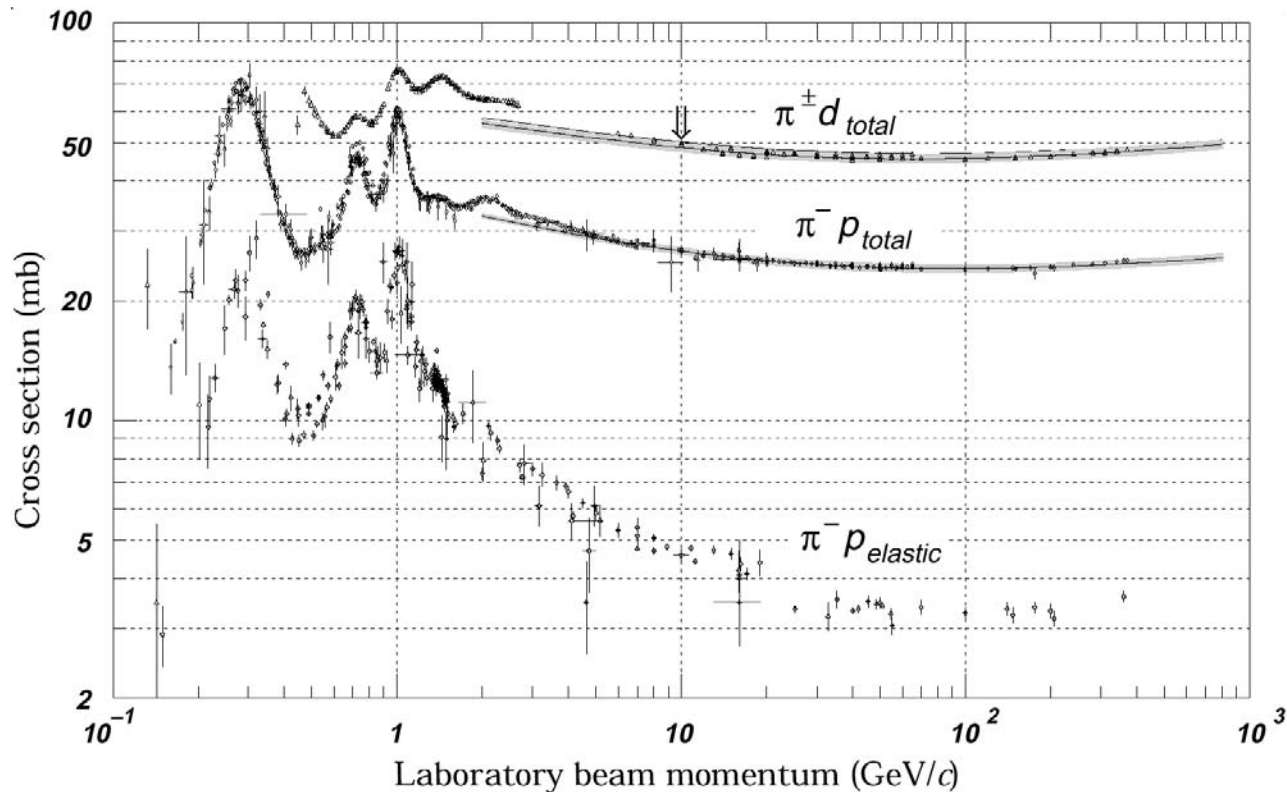


Figure 41: Cross sections of π^- on a fixed proton target

- ☉ For hadron-hadron scattering, cross-sections are of the same order with the geometrical “cross-sections” of hadrons: assuming their sizes are of order $r=1\text{ fm} \equiv 10^{-15}\text{ m} \Rightarrow \pi r^2 \approx 30\text{ mb}$
- ☉ For complex nuclei, cross-sections are bigger, and elastic scattering on a nucleon can cause nuclear excitation or break-up – *quasi-elastic scattering*

Knowing cross-sections and number of nuclei per unit volume in a given material n , one can introduce two important characteristics:

⊙ *nuclear collision length*: mean path between collisions, $l_c \equiv 1/n\sigma_{\text{tot}}$

⊙ *nuclear absorption length*: mean path between inelastic collisions, $l_a \equiv 1/n\sigma_{\text{inel}}$

At high energies, short-range nuclear interactions involve mainly hadrons, facilitating their detection.

Neutrinos and photons have much smaller cross-sections of interactions with nuclei, since former interact only weakly and latter – only electromagnetically.

Ionization energy losses

❖ Energy loss per travelled distance : dE/dx

⊙ Important for all charged particles

⊙ Mostly due to Coulomb scattering of particles off atomic electrons

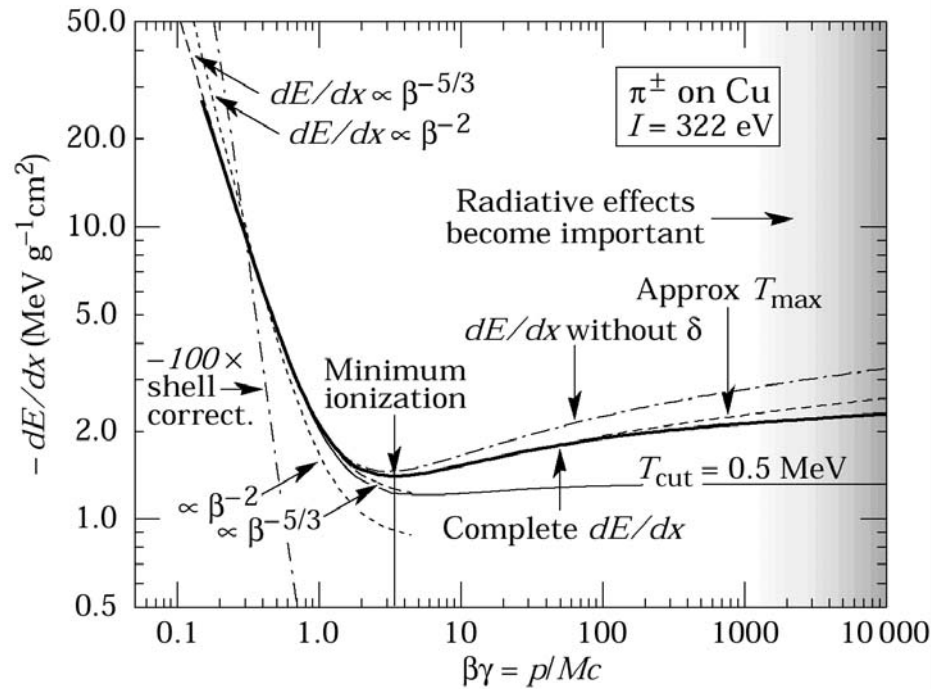


Figure 42: Energy loss rate for pions in copper. At low β , dE/dx is proportional to $1/\beta^2$. At high β , dE/dx proportional to $\ln(\beta)$

Bethe-Bloch formula for spin-0 bosons with charge $\pm e$ (e.g. π^+ , π^- , K^+ , K^-):

$$-\frac{dE}{dx} = \frac{Dn_e}{\beta^2} \left[\ln \left(\left(\frac{2mc^2\beta^2\gamma^2}{I} \right) - \beta^2 - \frac{\delta(\gamma)}{2} \right) \right] \quad (31)$$

$$D = \frac{4\pi\alpha^2\hbar^2}{m} = 5.1 \times 10^{-25} \text{ MeV cm}^2$$

In Equation (34), $\beta=v/c$ is velocity ($p=mv$); n_e , I and $\delta(\gamma)$ are constants which are characteristic to the medium:

- ⊙ n_e is the electron density, $n_e = \rho N_A Z / \tilde{A}$, where ρ is the mass density of the medium and \tilde{A} is its atomic weight. Hence, energy loss is strongly *proportional to the density* of the medium
- ⊙ I is the mean ionization potential, $I \approx 10Z \text{ eV}$ for $Z > 20$
- ⊙ $\delta(\gamma)$ is a dielectric screening correction, important only for very energetic particles.

Radiation energy losses

- ❖ Electric field of a nucleus accelerates or decelerates particles, causing them to radiate photons, hence, lose energy: *bremstrahlung* (literally, “braking radiation”)

Bremstrahlung is an important source of energy loss for light particles. It is, however, significant only for high-energy electrons and positrons.

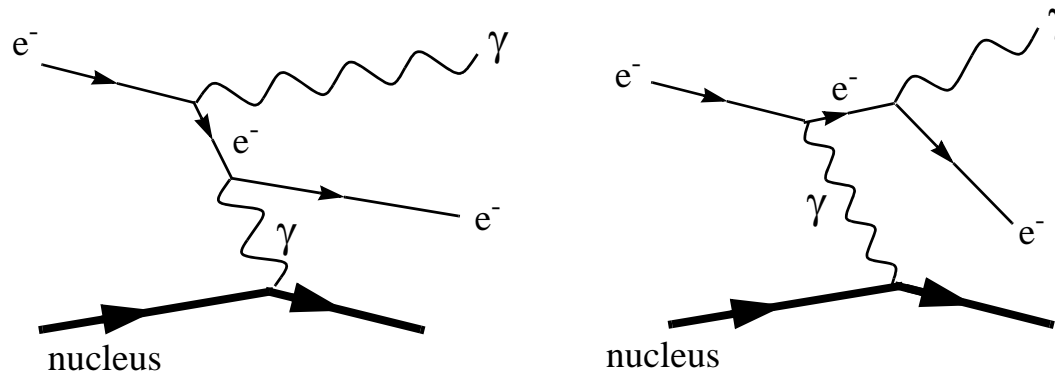


Figure 43: Dominant Feynman diagrams for a bremsstrahlung process
 $e^- + (Z,A) \rightarrow e^- + \gamma + (Z,A)$

⊙ Contribution to bremsstrahlung from nucleus field is of order $Z^2\alpha^3$, and from atomic electrons – of order $Z\alpha^3$ (α^3 from each electron).

⊙ For relativistic electrons, average rate of bremsstrahlung energy loss is given by:

$$-\frac{dE}{dx} = \frac{E}{L_R} \quad (32)$$

The constant L_R is called the **radiation length**:

$$\frac{1}{L_R} = 4 \left(\frac{\hbar}{mc} \right)^2 Z(Z+1) \alpha^3 n_a \ln \left(\frac{183}{Z^{1/3}} \right) \quad (33)$$

In Equation (33), n_a is the density of atoms per cm^3 in medium.

- ❖ Radiation length is the average thickness of material which reduces mean energy of a particle (electron or positron) by factor e .

Interactions of photons in matter

Main contributing processes to the total cross-section of photon interaction with atom are:

- ☉ Photoelectric effect ($\sigma_{p.e.}$)
- ☉ Compton scattering (σ_{incoh})
- ☉ Pair production in nuclear and electron field (κ_N and κ_e)



Figure 44: Photoelectric effect (left) and Compton scattering (right)

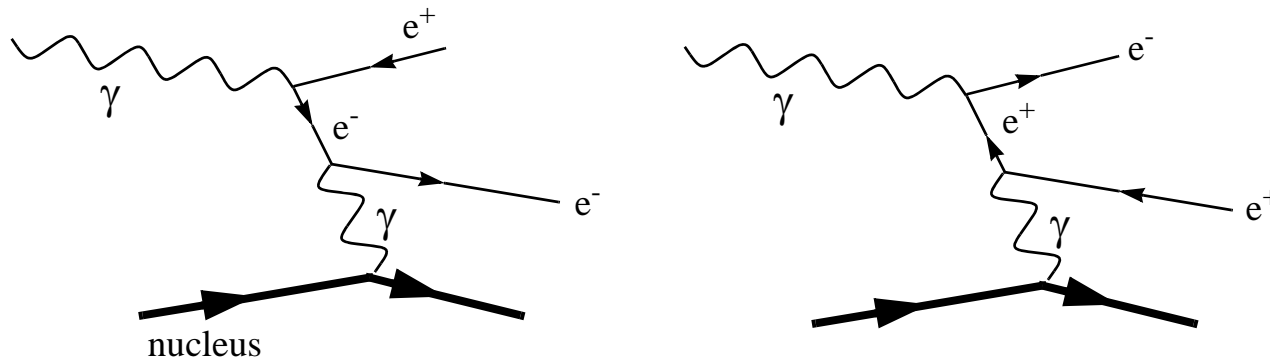


Figure 45: Pair production

At high energies, pair production is the dominant process: $\sigma_{\text{pair}} = \frac{7}{9} n_a L_R$, and number of photons travelled distance x in matter is

$$I(x) = I_0 e^{-7x/9L_R}$$

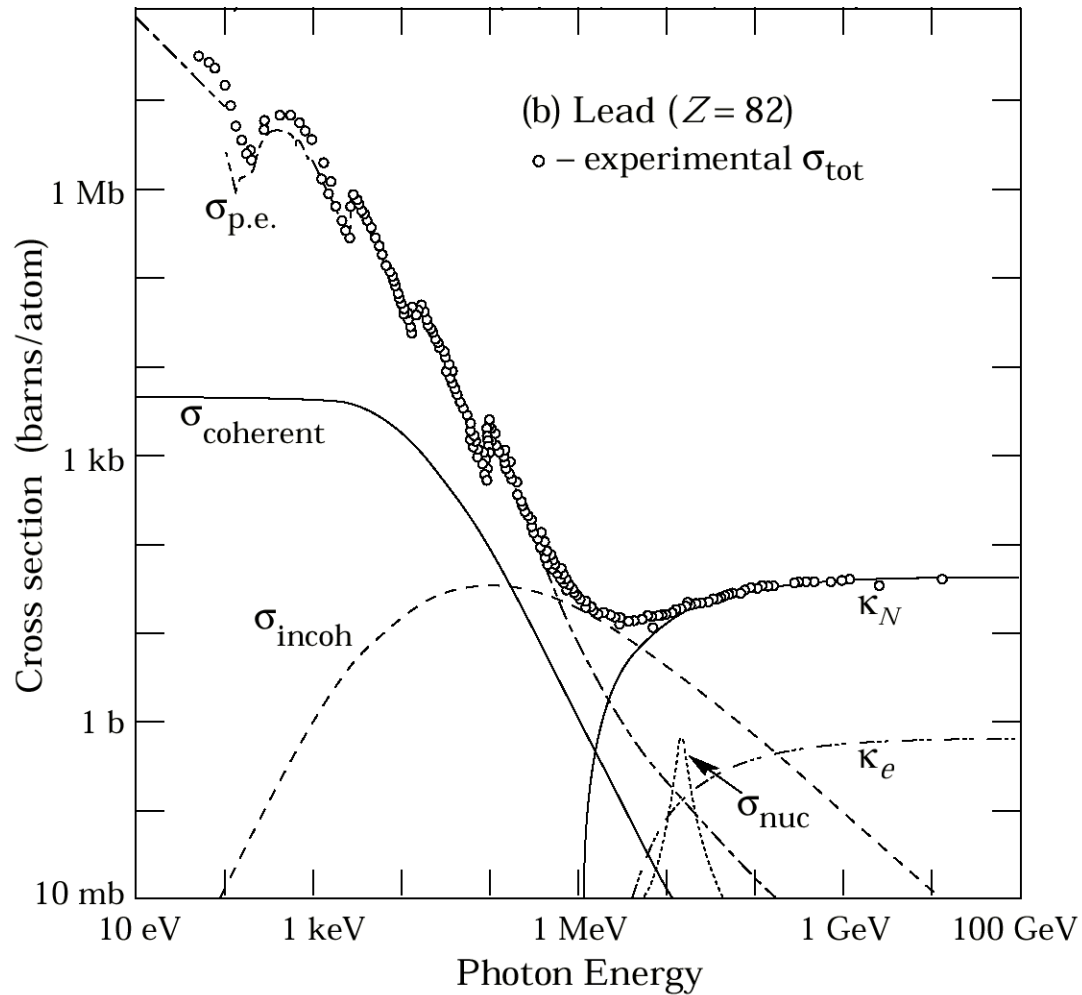


Figure 46: Photon interaction cross-section on a lead atom

☉ Note that pair production occurs when photon energies reach $E > 2m_e$ ($E > 1 \text{ MeV}$).

Particle detectors

Particle detectors consist of many subsystems:

- 1) Tracking devices – coordinate measurements
- 2) Calorimeters – energy measurements
- 3) Time resolution counters
- 4) Particle identification devices
- 5) Spectrometers – momentum measurements

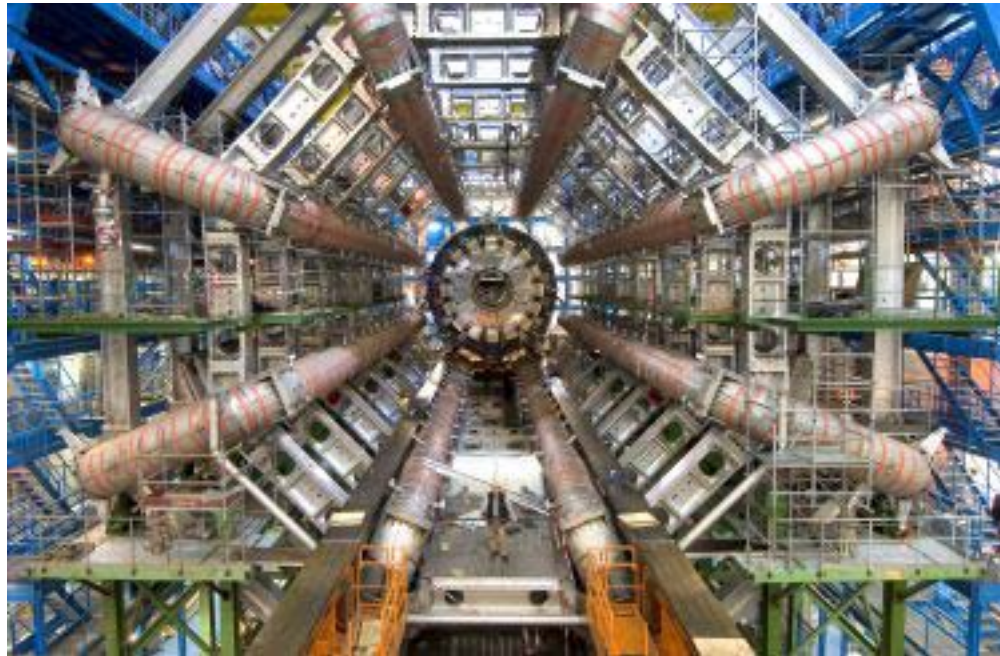


Figure 47: Assembly of the ATLAS detector

Position measurement

- ❖ Main principle: ionization products are either visualized (as in photoemulsions) or collected on electrodes to produce an electronic signal, to be processed by a computer

Basic requirements of high-energy physics experiments:

- ⊙ High spatial resolution ($\propto 10\text{-}100\ \mu\text{m}$)
- ⊙ Possibility to register particles synchronously with a high rate (good *triggering*)

To fulfil the latter, electronic signal pick-up is necessary, therefore photoemulsions and bubble chambers were ultimately abandoned

- ❖ Modern tracking detectors fall in two major categories:
 - ⊙ Gaseous detectors (“*gas chambers*”), resolution $\sim 100\text{-}500\ \mu\text{m}$
 - ⊙ Semiconductor detectors, resolution $\sim 5\ \mu\text{m}$

Proportional and drift chambers

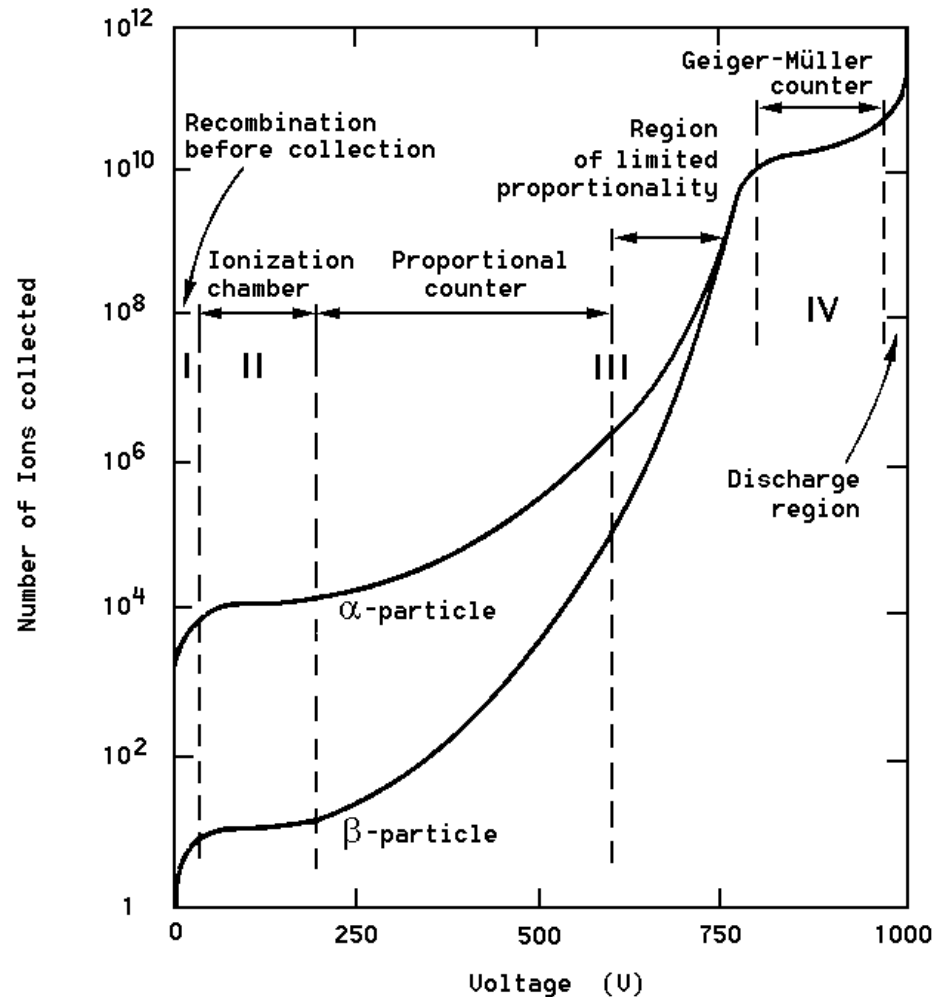


Figure 48: The number of electron-ion pairs collected when a charged particle traverses a gaseous detector of average size, as a function of applied voltage

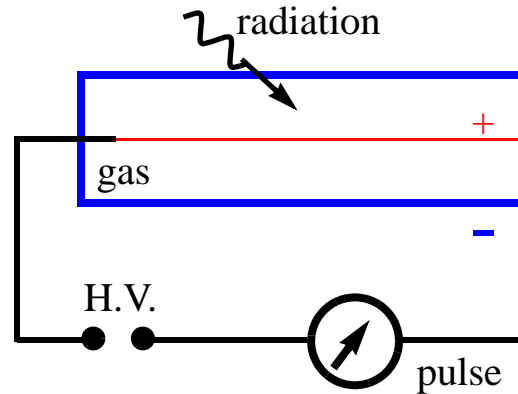


Figure 49: Basic scheme of a wire chamber

❖ A simplest proportional chamber:

- A conducting chamber, filled with a gas mixture, serves as a cathode itself, while the wire inside serves as an anode
- The field accelerates the electrons produced in ionization \Rightarrow secondary electron-ion pairs \Rightarrow avalanche of electrons \Rightarrow pulse in the anode. Amplification is $\propto 10^5$ for voltage of 10^4 - 10^5 V/cm. Gas mixture is adjusted to limit the avalanche.

🎯 Several anode wires \Rightarrow coordinate measurement possibility (*Multi-Wire Proportional Chamber*, MWPC)

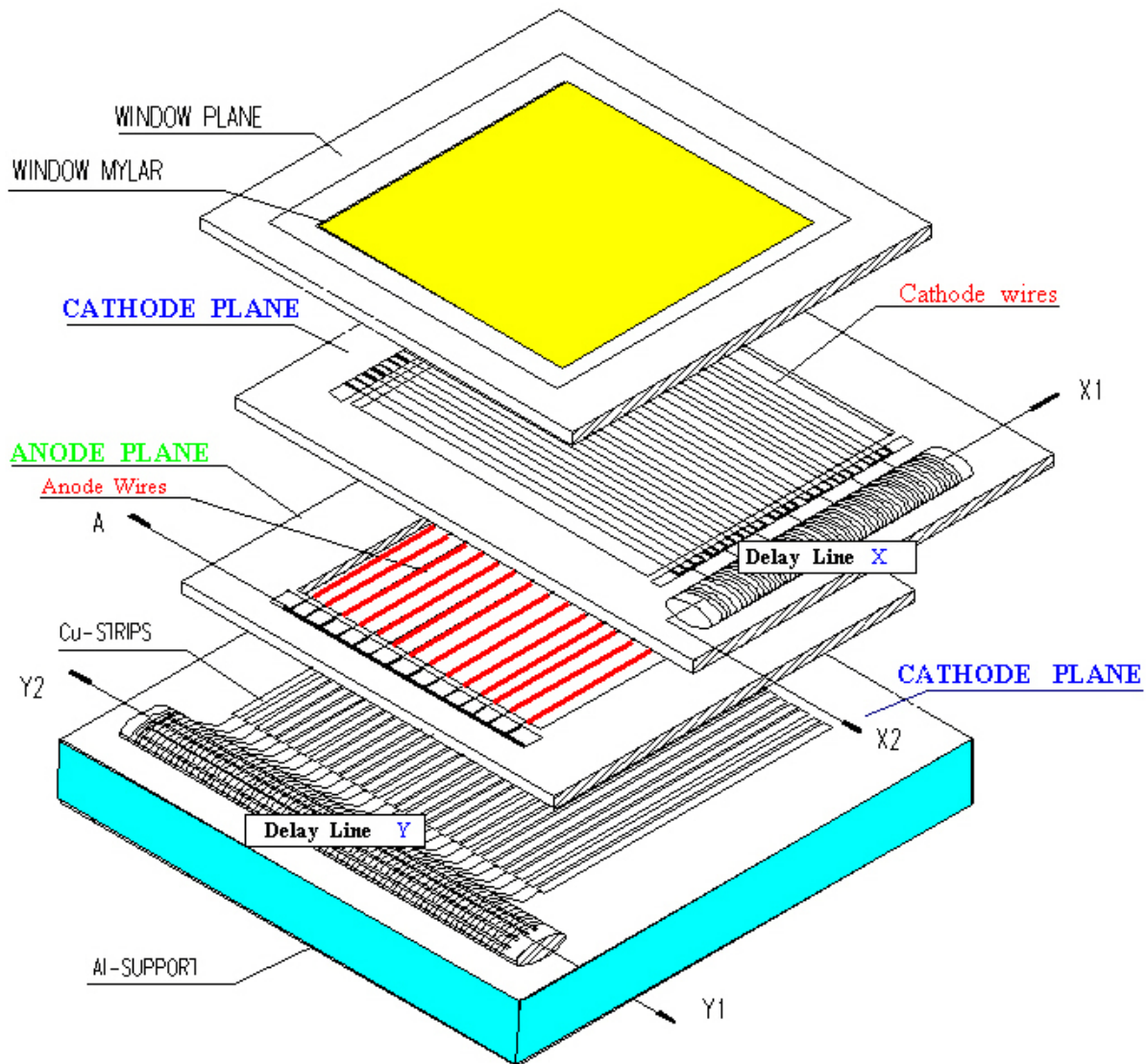


Figure 50: Common view of the 2-dimensional MWPC

❖ Alternative to MWPC : *drift chambers*

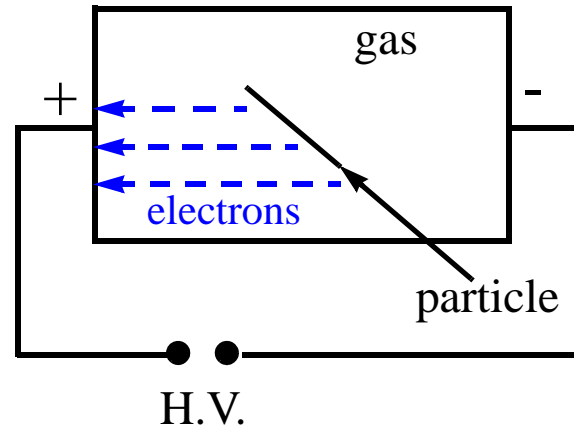


Figure 51: Basic scheme of a drift chamber

- Ionization electrons produced along the particle passage arrive to the pick-up anode at different times t_1, t_2, t_3, \dots
- knowing (from other detectors) the time of particle's arrival t_0 and field in the chamber, one can calculate coordinates of the track l_1, l_2, l_3, \dots
- ⊙ *Streamer detectors* are wire chambers in which secondary ionization is not limited and develops into moving plasmas – *streamers*
- ⊙ If H.V. pulse in a chamber is long enough, a spark will occur: *spark chambers*

Semiconductor detectors

- ❖ In semiconducting materials, ionizing particles produce electron-hole pair. Number of these pairs is proportional to energy loss by particles

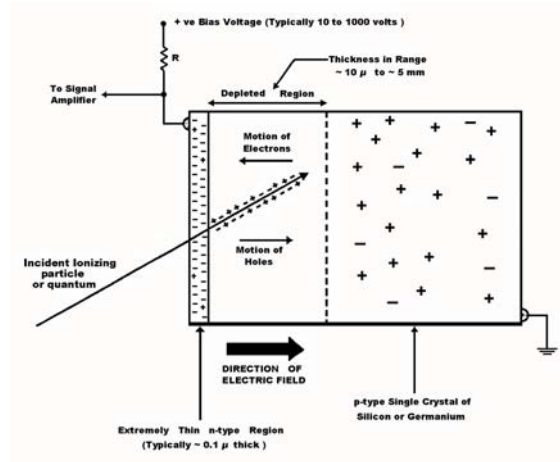


Figure 52: Typical silicon detector is a p-n junction diode operated at reverse bias

- ⊙ Superior resolution (few μm), small size, small power consumption, fast signals.
- ⊙ Subject to radiation damages; can be circumvented by using radiation-hard manufacturing processes, appropriate handling (e.g. cooling) and by using very thin detectors.

Calorimeters

- ❖ To measure energy (and position) of the particle, calorimeters use absorbing material to capture all the energy of the particle.
- ❖ Signals produced in calorimeters are proportional to the energy of the incoming particle.
- ❖ During the absorption process, particle interacts with the material of the calorimeter and produces a secondary *shower* of particles.
- ❖ Since *electromagnetic* and *hadronic* showers are somewhat different, there are two corresponding types of calorimeters

Electromagnetic calorimeters

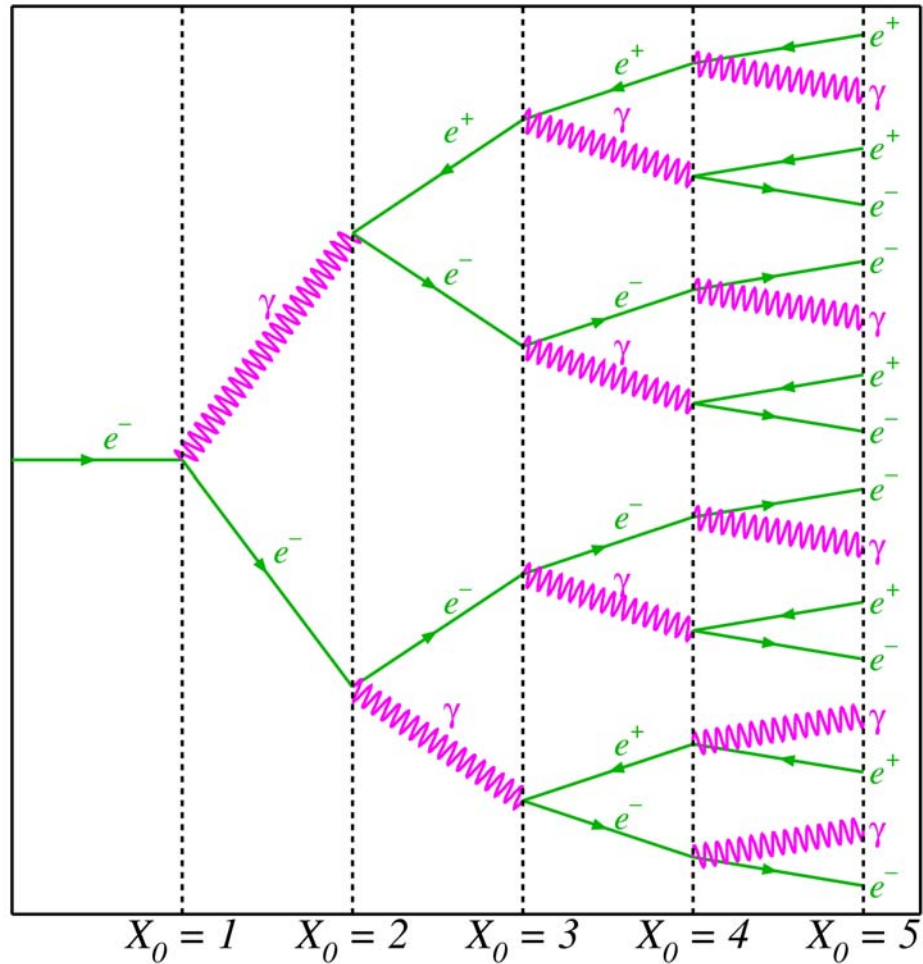


Figure 53: Electromagnetic shower; depth in radiation lengths

❖ Used for electron/positron and γ energy measurements

- ⊙ Dominant energy loss for high-energy electrons (or positrons) is bremsstrahlung:
 $e^- \rightarrow e^- \gamma$
- ⊙ Photons produced via bremsstrahlung produce e^+e^- pairs and are thus absorbed again: $\gamma \rightarrow e^+e^-$
- ⊙ An initial electron thus produces a cascade of photons and e^+e^- pairs, until its energy falls under the bremsstrahlung threshold of $E_C \approx 600 \text{ MeV}/Z$

❖ A calorimeter has to be large enough to absorb all the possible energy of the incoming particle.

Main assumptions for electromagnetic showers:

- Each electron with $E > E_C$ travels one radiation length and radiates a photon with $E_\gamma = E/2$
- Each photon with $E_\gamma > E_C$ travels one radiation length and creates an e^+e^- pair, which shares equally E_γ
- Electrons with $E < E_C$ cease to radiate; for $E > E_C$ ionization losses are negligible

These considerations lead to the expression:

$$t_{max} = \frac{\ln(E_0/E_C)}{\ln 2} \quad (34)$$

where t_{max} is number of radiation lengths needed to stop the electron of energy E_0 .

Electromagnetic calorimeters can be, for example, lead-glass (crystal) blocks collecting the light emitted by showers, or a drift chamber interlayed with heavy absorber material (lead).

Hadron calorimeters

- ❖ Used for hadron energy measurement (π , K , protons, neutrons)
 - ☉ Hadronic showers are similar to the electromagnetic ones, but absorption length is larger than the radiation length of electromagnetic showers since hadrons interact in the material through nuclear interactions.
 - ☉ Also, some contributions to the total absorption may not lead to a signal in the detector (e.g., nuclear excitations or secondary neutrinos)

Main characteristics of a hadron calorimeter are:

- (a) It has to be thicker than electromagnetic one
 - (b) Layers of ^{238}U can be introduced to compensate for energy losses (low-energy neutrons cause fission)
 - (c) energy resolution of hadron calorimeters is generally rather poor
- ❖ Hadron calorimeter is usually a set of MWPC's or streamer tubes, interlayed with thick iron absorber

Scintillation counters

- ❖ Scintillation counters are widely used to detect the passage of charged particles through an experimental setup and to measure particle's "*time-of-flight*" (TOF).
- ❖ Scintillators are materials (crystals or organic) in which ionizing particles produce visible light without losing much of its energy
 - ☉ The light is guided down to photomultipliers and is being converted to a short electronic pulse.

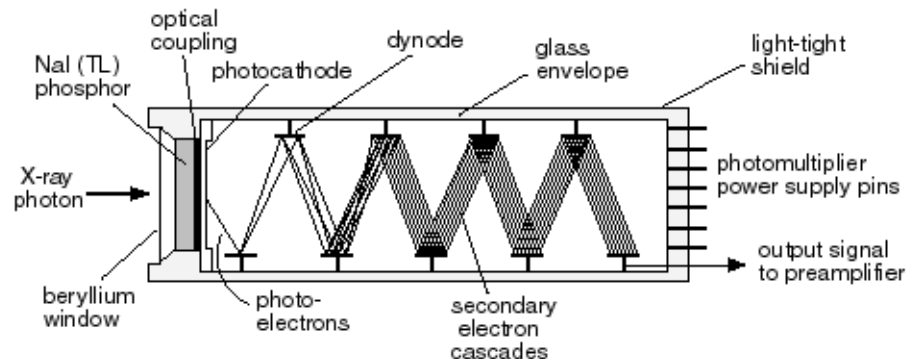


Figure 54: Scheme of a scintillation detector and photomultiplier assembly

Particle identification

- ⊙ Particles are identified by mass and charge: knowing momentum of particle is not enough to find those out, complementary information is needed.
 - ⊙ For low-energy particles ($E < 1 \text{ GeV}$), TOF counters can provide this complementary data.
 - ⊙ Energy loss rate dE/dx depends on particle mass for energies below $\approx 2 \text{ GeV}$ ($1/\beta^2$ region of Bethe-Bloch formula)
- ❖ The most reliable particle identification device: *Cherenkov counters*
- ⊙ In certain media, energetic charged particles move with velocities higher than the speed of light in these media
 - ⊙ Excited atoms along the path of the particle emit coherent photons at a characteristic angle θ_C to the direction of motion

The angle θ_C depends on the refractive index of the medium n and on the particle's velocity v :

$$\cos\theta_C = c/vn \quad (35)$$

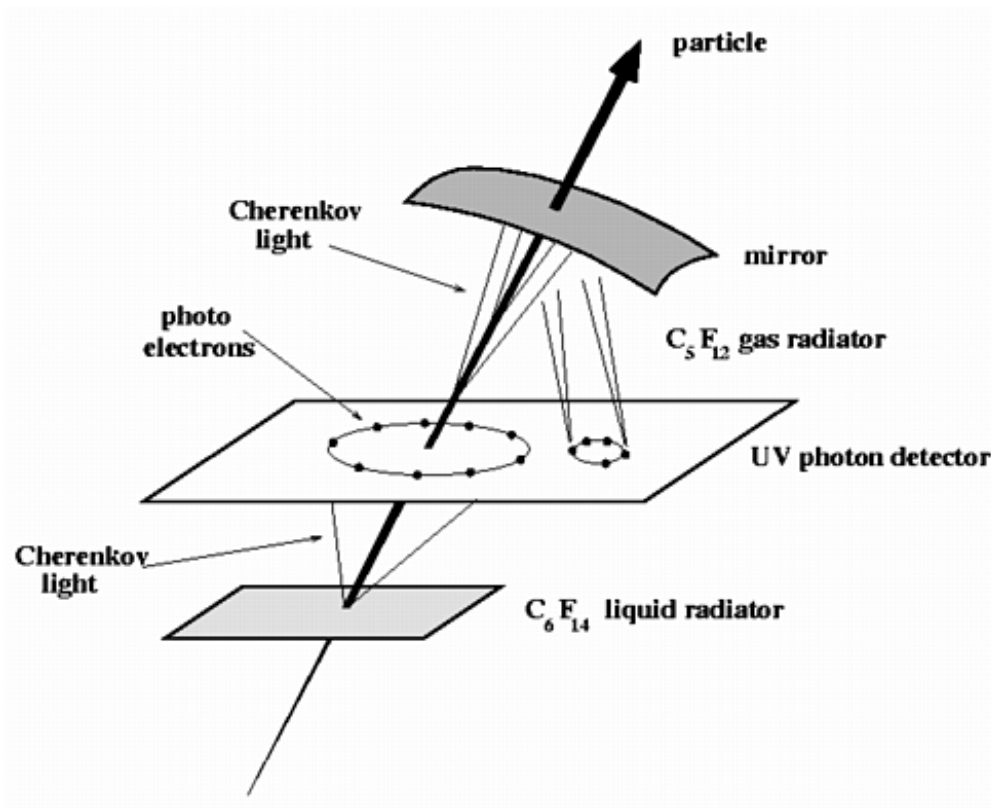


Figure 55: Cherenkov effect in the DELPHI RICH detector

- ☉ Measuring θ_C , the velocity of the particle can be easily derived, and the identification performed: p is measured by a tracking device, v by the Cherenkov counter $\Rightarrow m=p/v$.

Transition radiation measurements

- ⊙ In ultra-high energy region, particles velocities do not differ very much
- ⊙ Whenever a charged particle traverses a border between two media with different dielectric properties, a *transition radiation* occurs
- ⊙ Intensity of emitted radiation is sensitive to the particle's energy $E = \gamma mc^2$.
- ⊙ Transition radiation occurs only if $\gamma > 1000$, which means $E/m > 1000$.

Transition radiation measurements are particularly useful for separating electrons from other particles: for electrons, $\gamma = 1000$ for $E = 0.5 \text{ GeV}$. For pions, $\gamma = 1000$ for $E = 135 \text{ GeV} \Rightarrow e/\pi$ separation between 0.5 and 135 GeV.

Spectrometers

- ❖ Momenta of particles can be measured by curvatures of tracks in a magnetic field: $p = 0.3B\rho$, where ρ is curvature, B is magnetic field.

Spectrometers are tracking detectors placed inside a magnet, providing momentum information

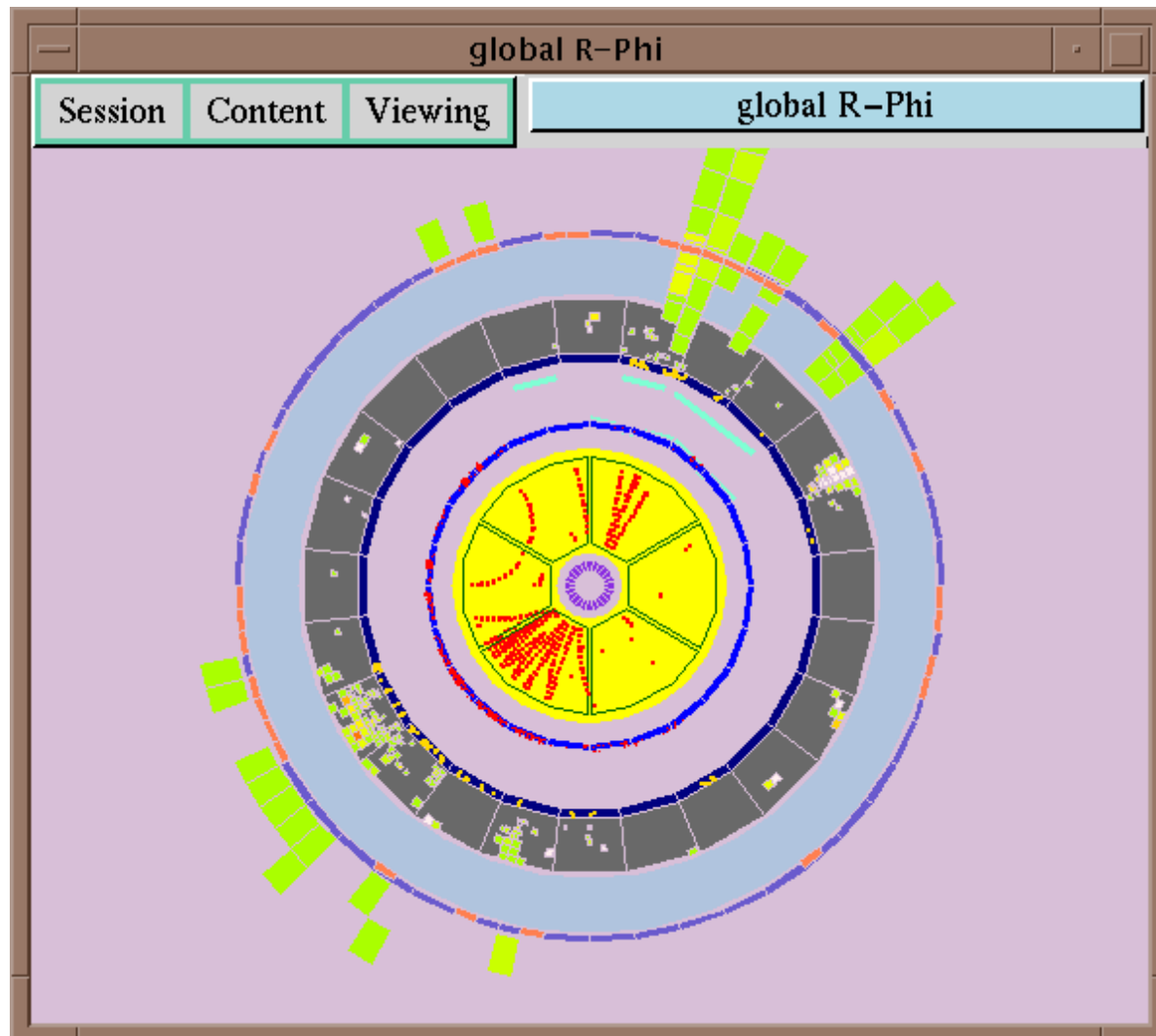


Figure 56: A e^+e^- annihilation event as seen by the DELPHI detector. In collider experiments, all the tracking setup is typically contained inside a solenoidal magnet.

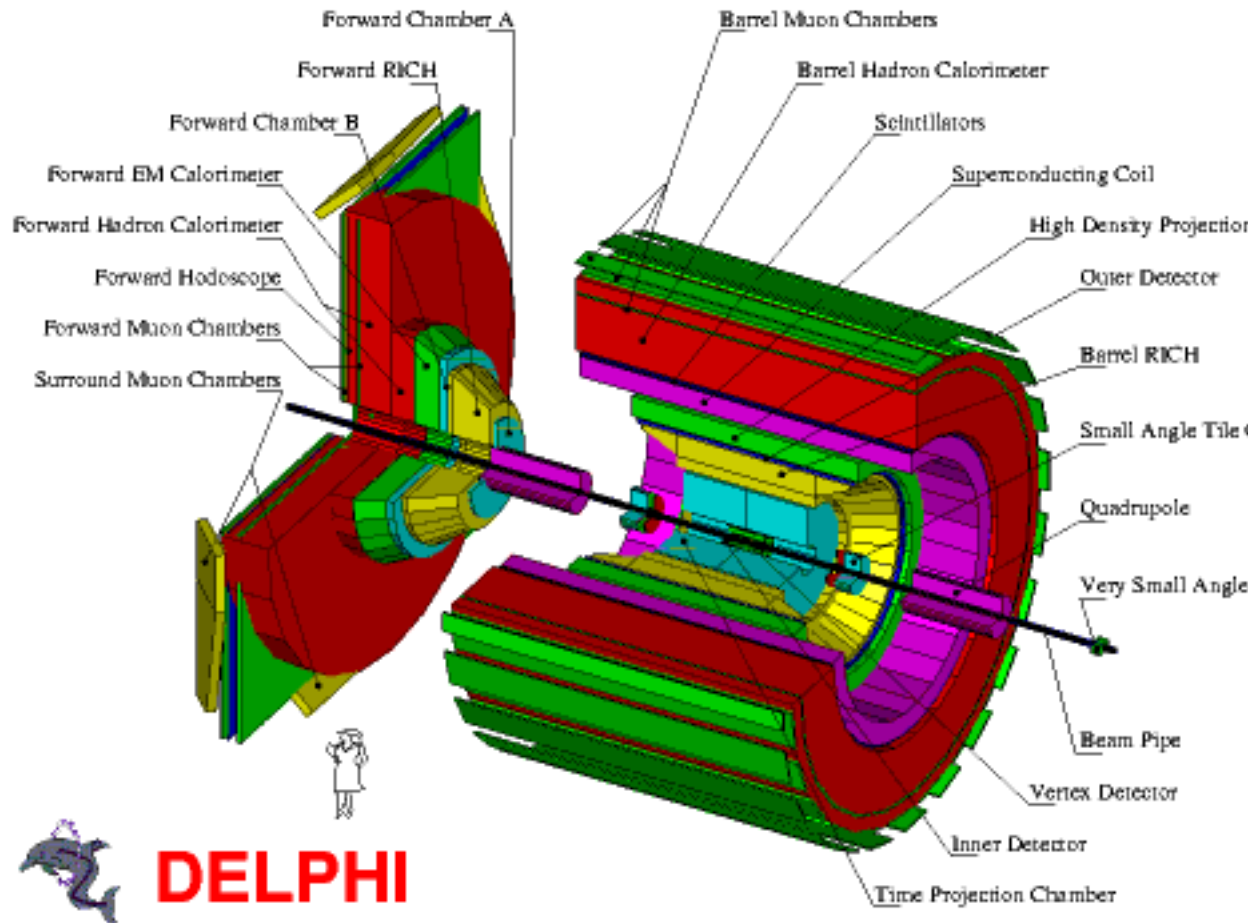


Figure 57: The DELPHI detector at LEP (operated in 1989 - 2001)
~10 meters long, 3500 tons

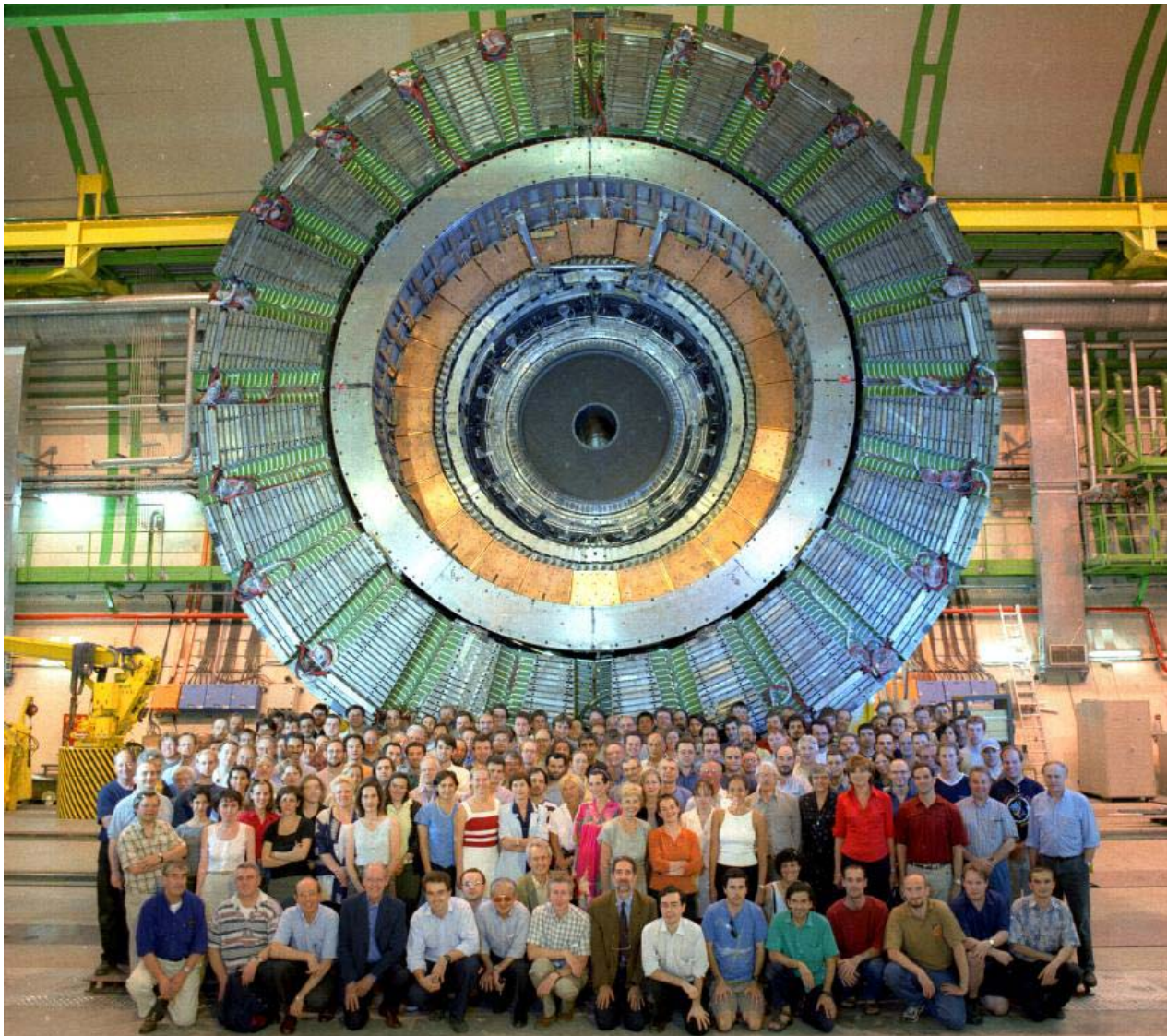


Figure 58: DELPHI detector being disassembled

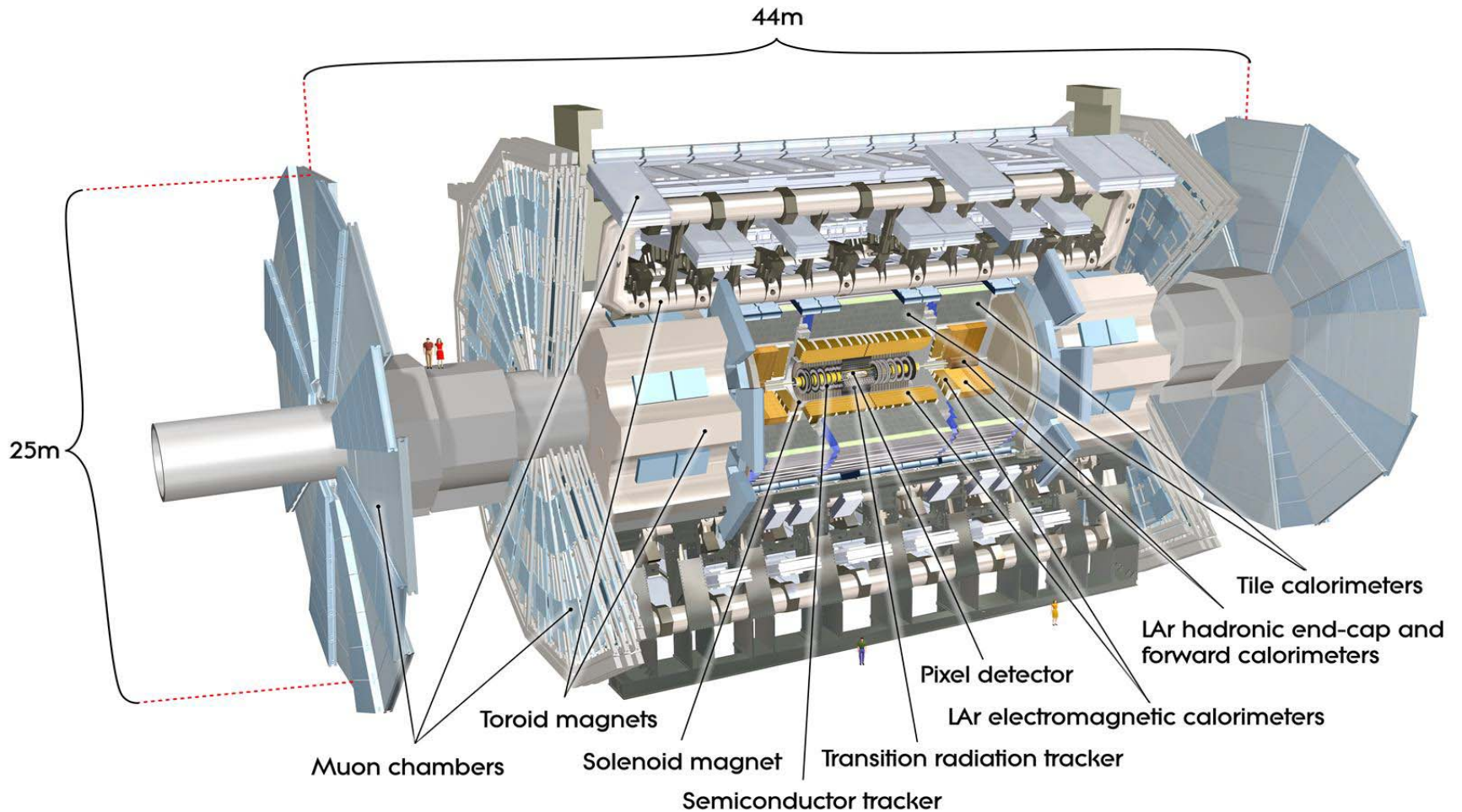


Figure 59: ATLAS detector at LHC, operates since 2008
44m long, 7000 tons

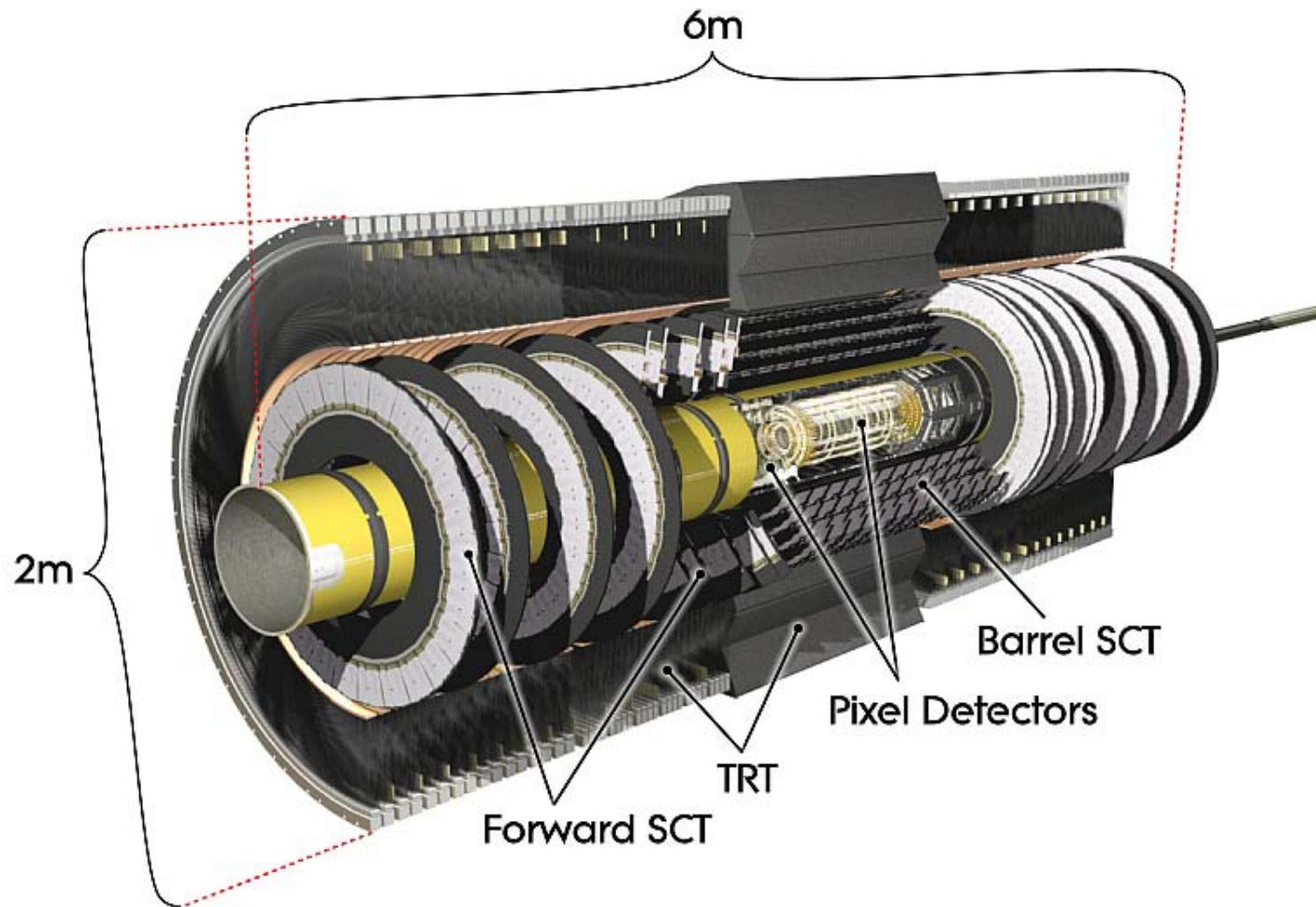


Figure 60: ATLAS Inner Detector: semiconductor trackers and the transition radiation tracker

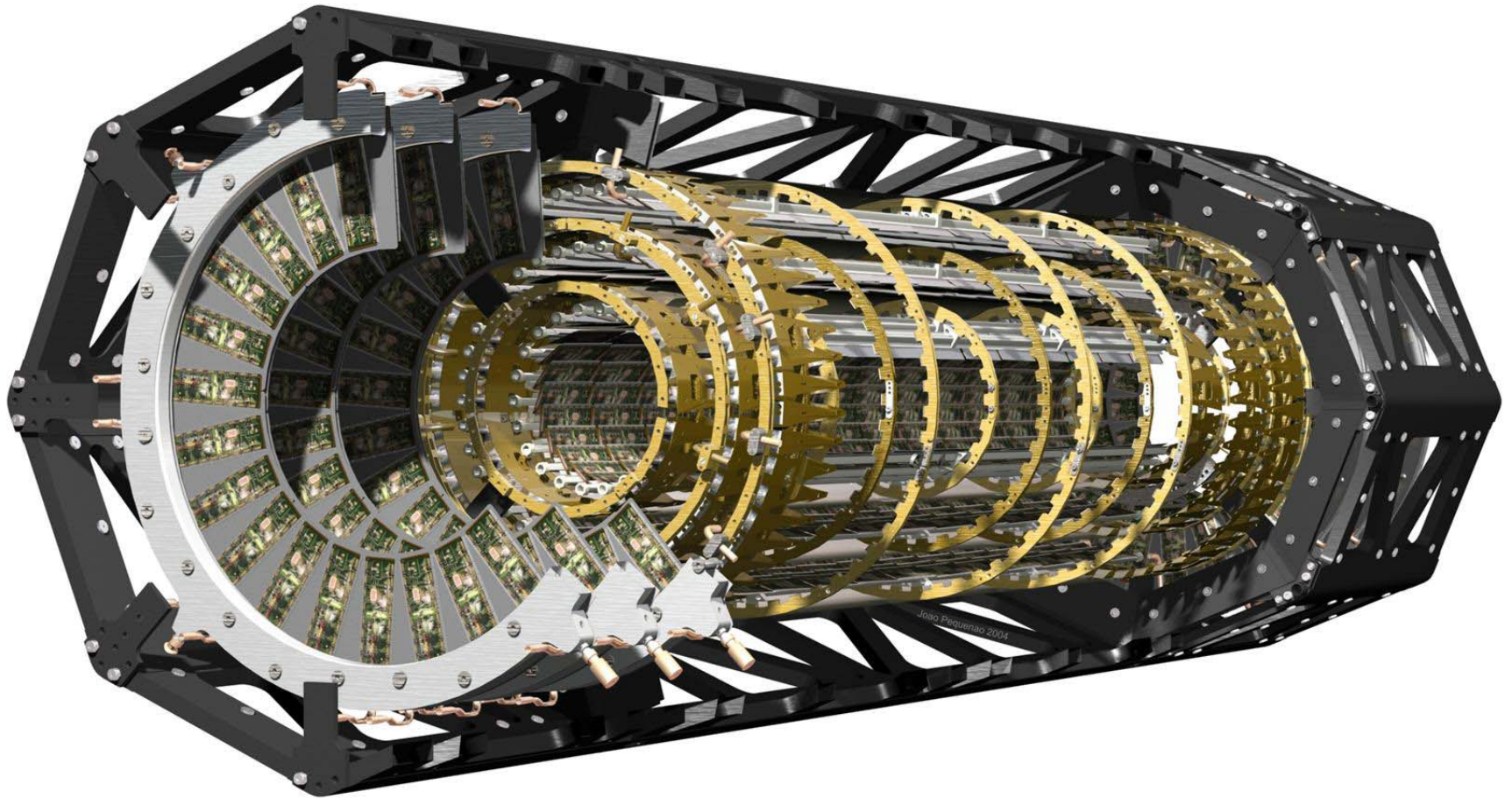


Figure 61: ATLAS Pixel Detector close-up

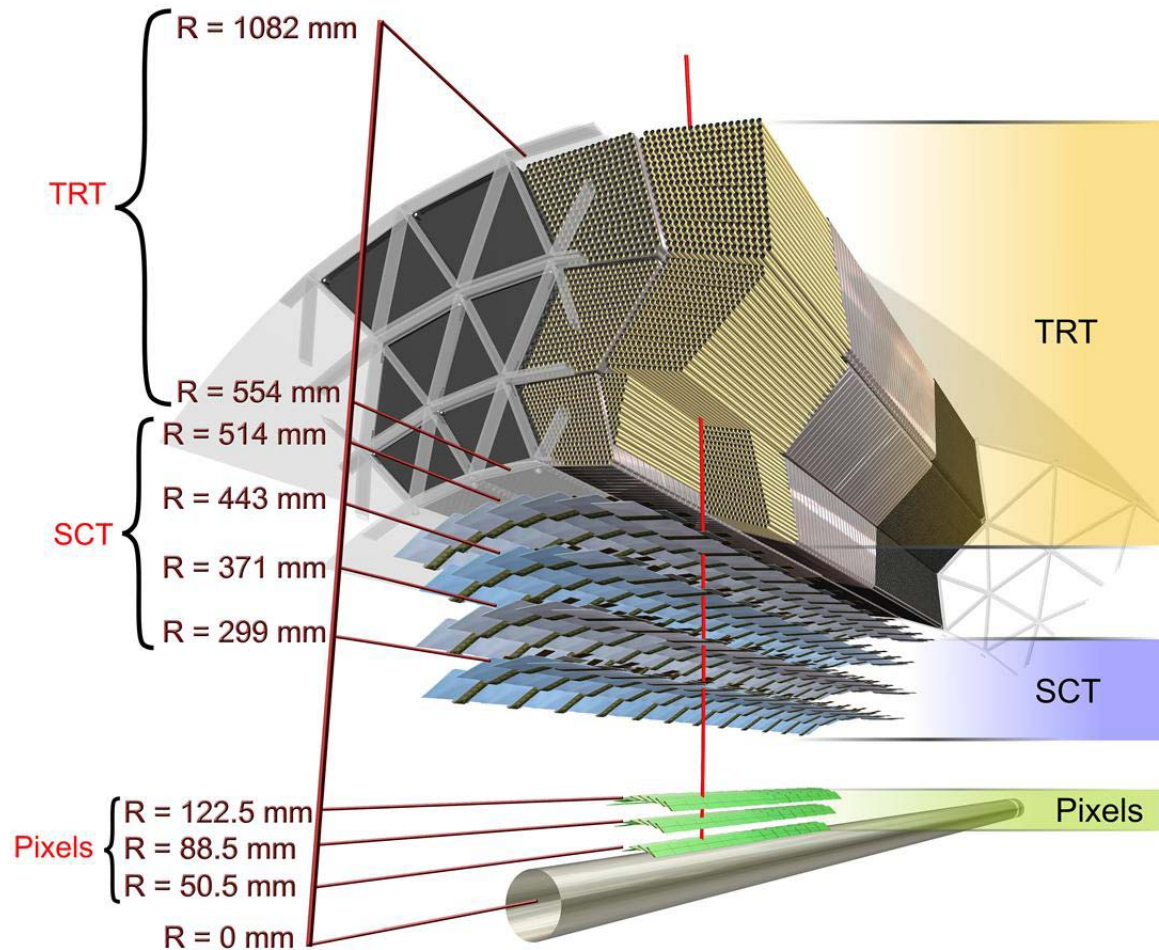


Figure 62: ATLAS inner trackers as seen by a particle

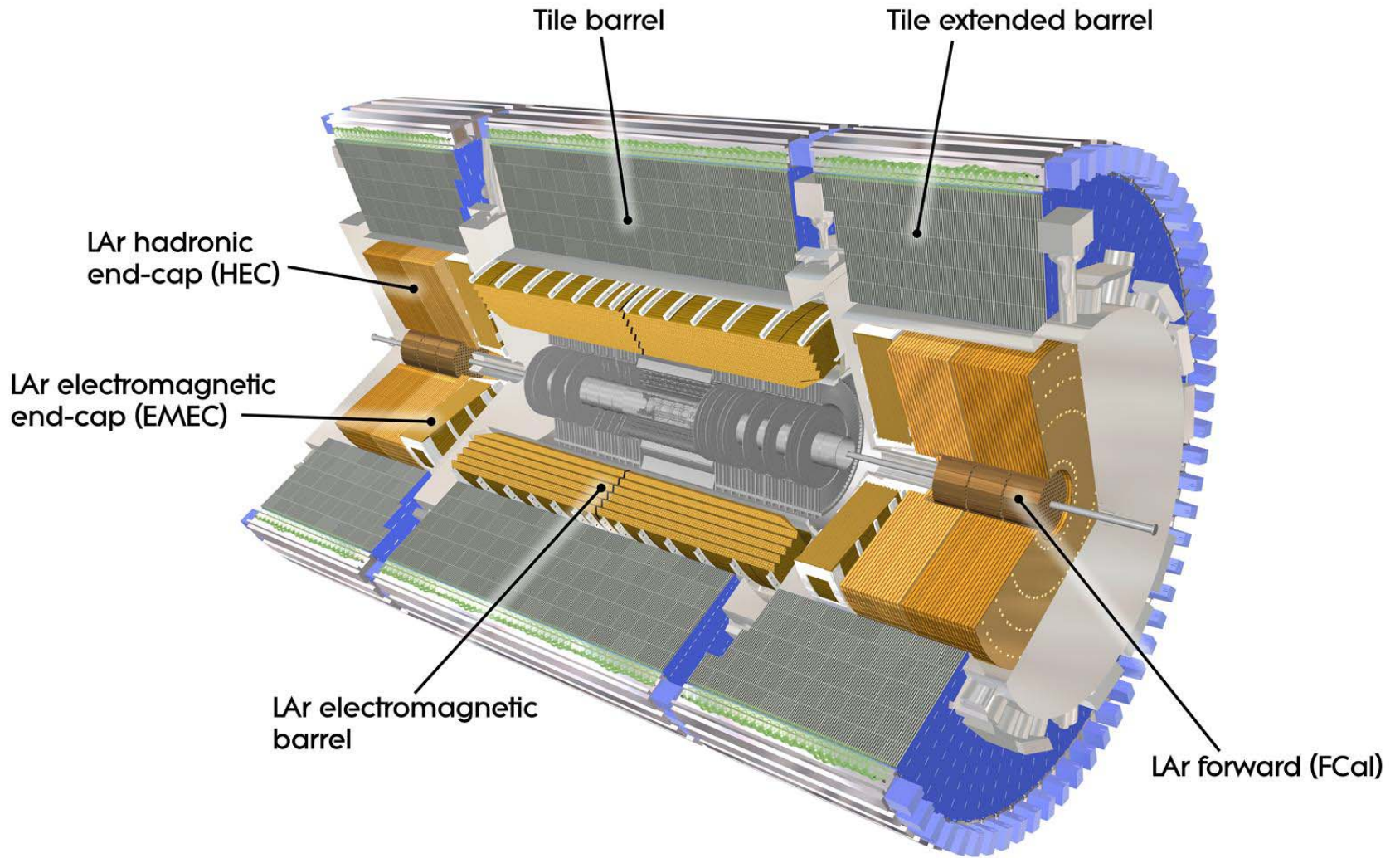


Figure 63: ATLAS calorimeters. LAr (for “liquid Argon”): EM and hadronic (absorbers: lead, copper, tungsten). TileCAL - hadronic, steel/scintillator

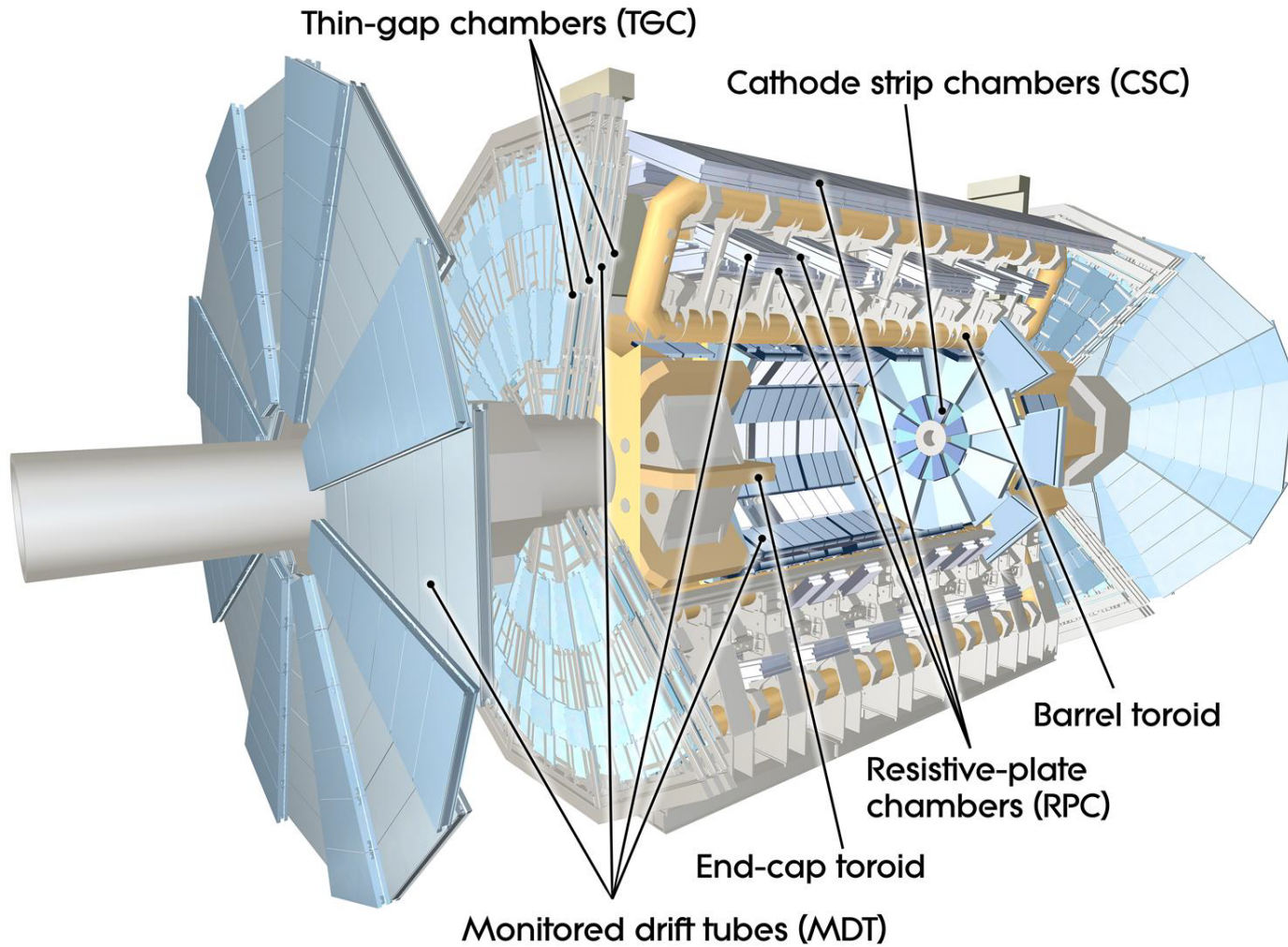


Figure 64: ATLAS muon systems



Figure 65: ATLAS solenoid (left) and end-cap toroid (right)

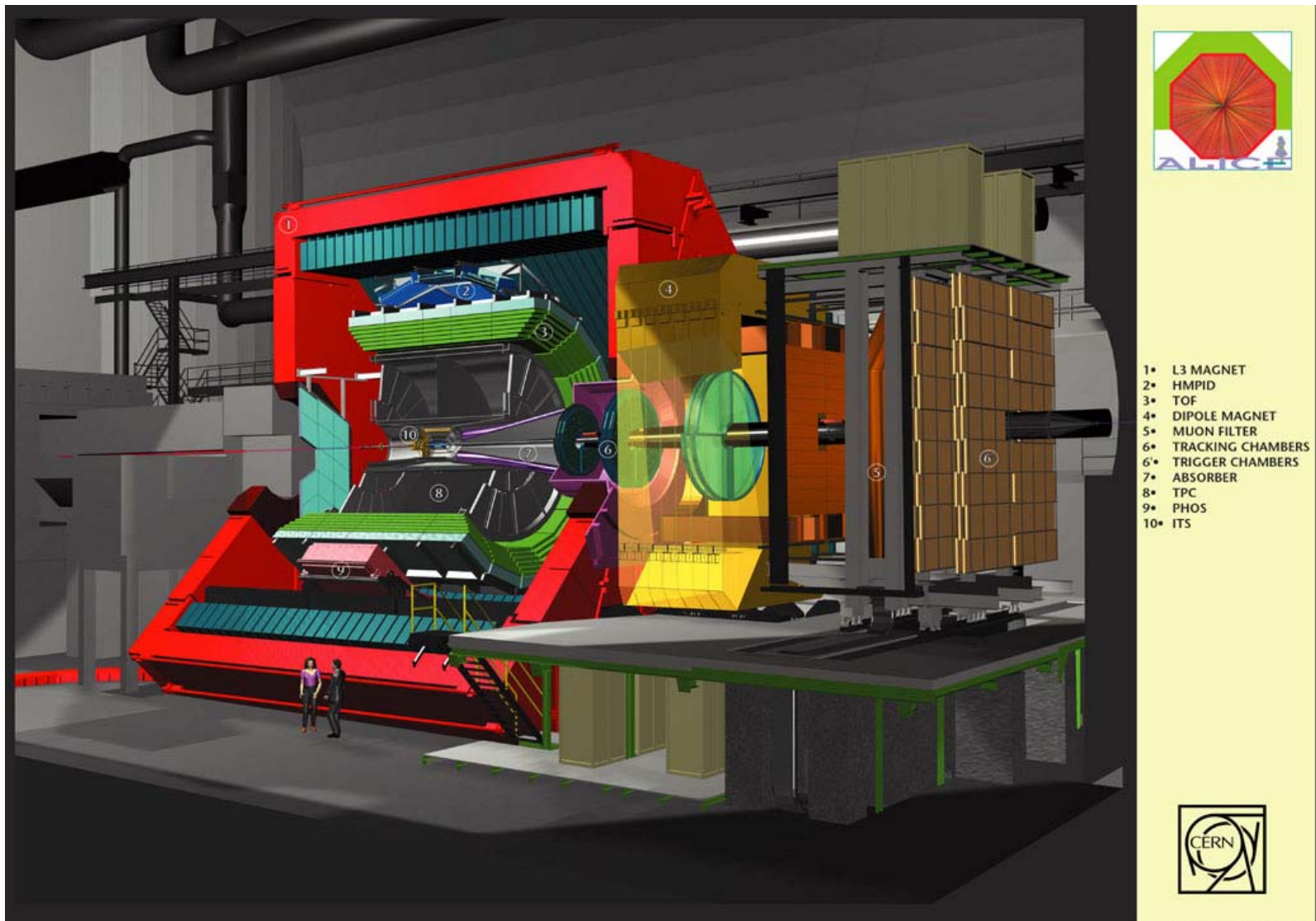


Figure 66: ALICE detector at LHC - dedicated to Pb-Pb collision measurements

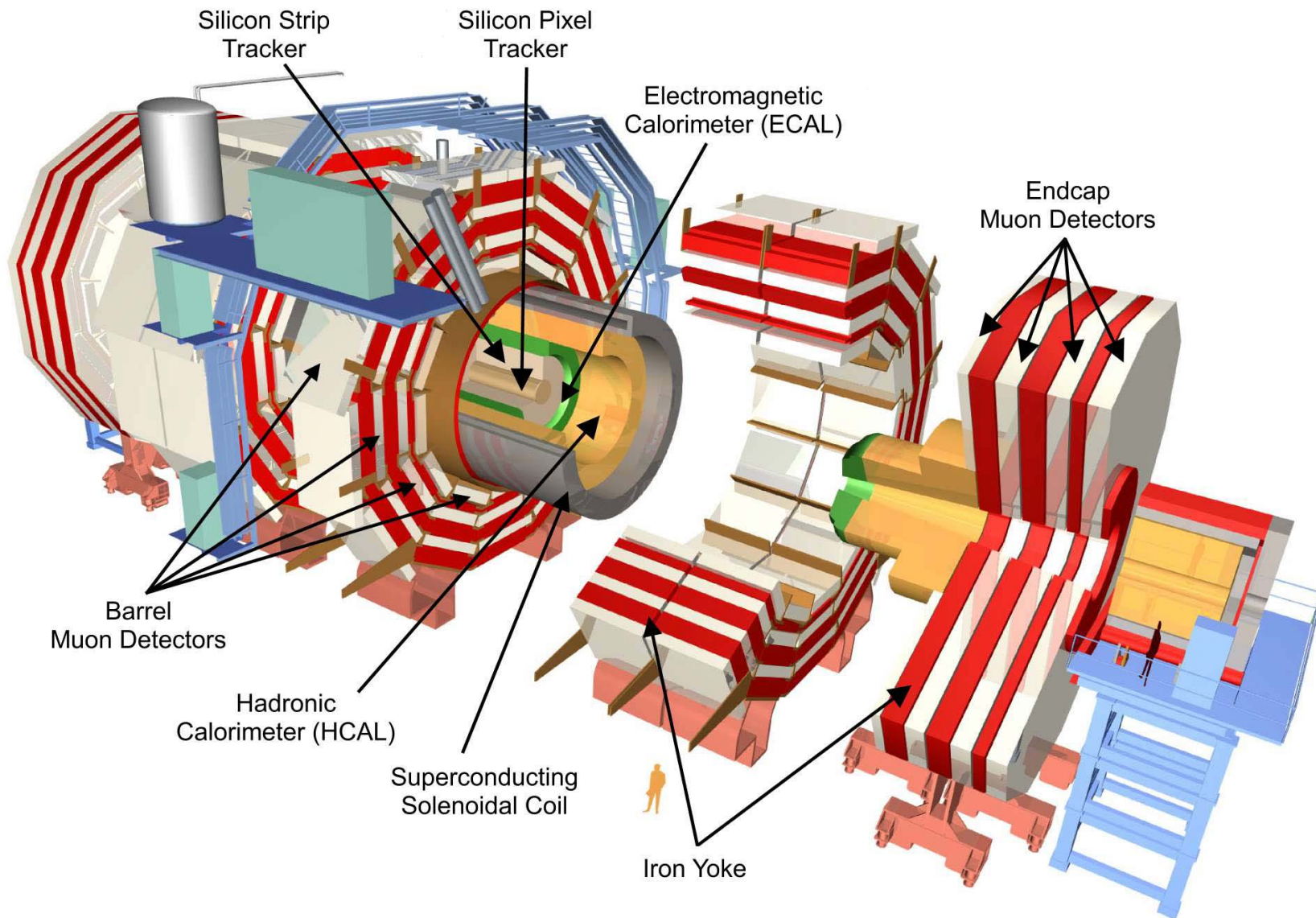


Figure 67: CMS detector at LHC

LHC-B Detector

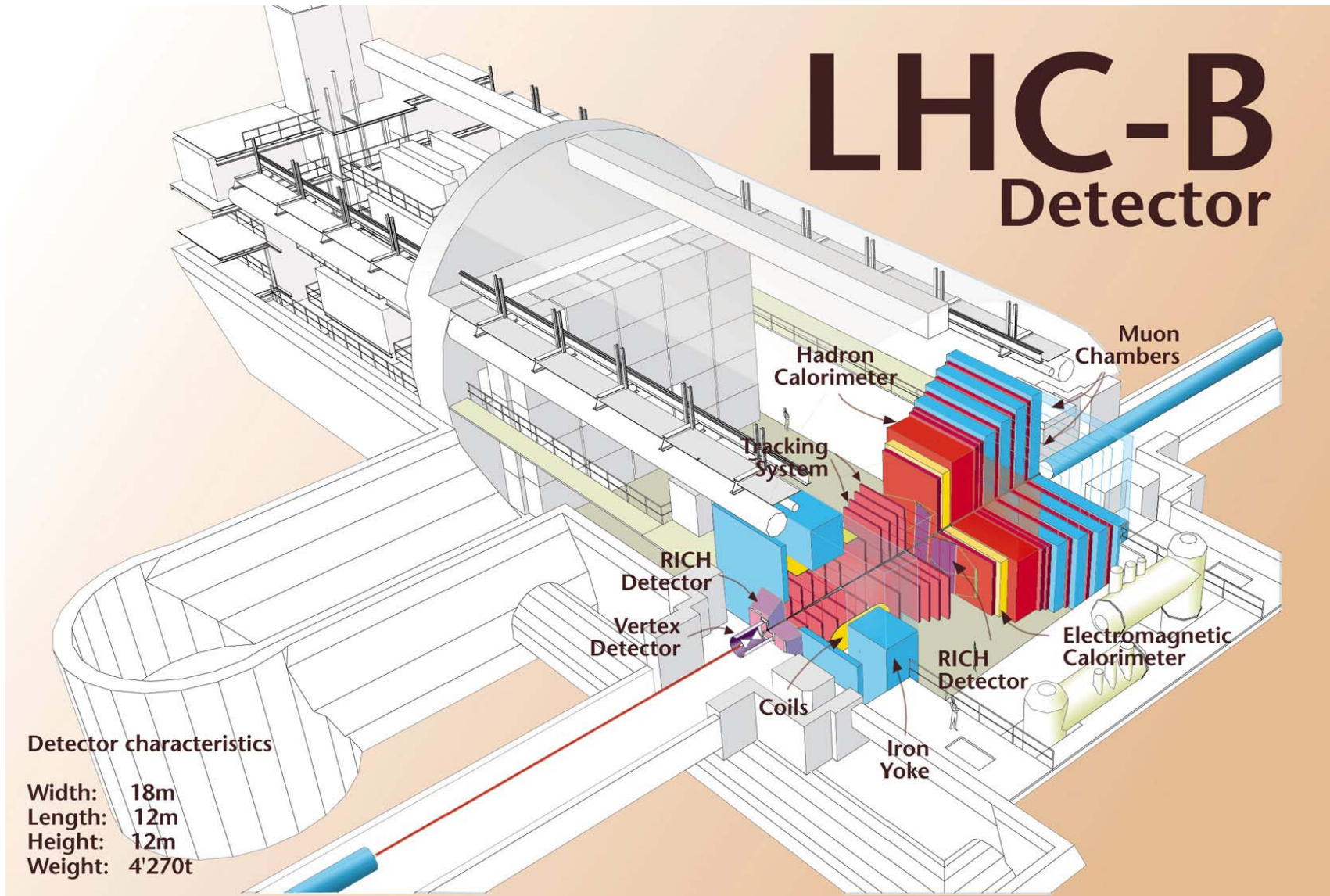


Figure 68: LHC-b detector at LHC, dedicated to B meson studies

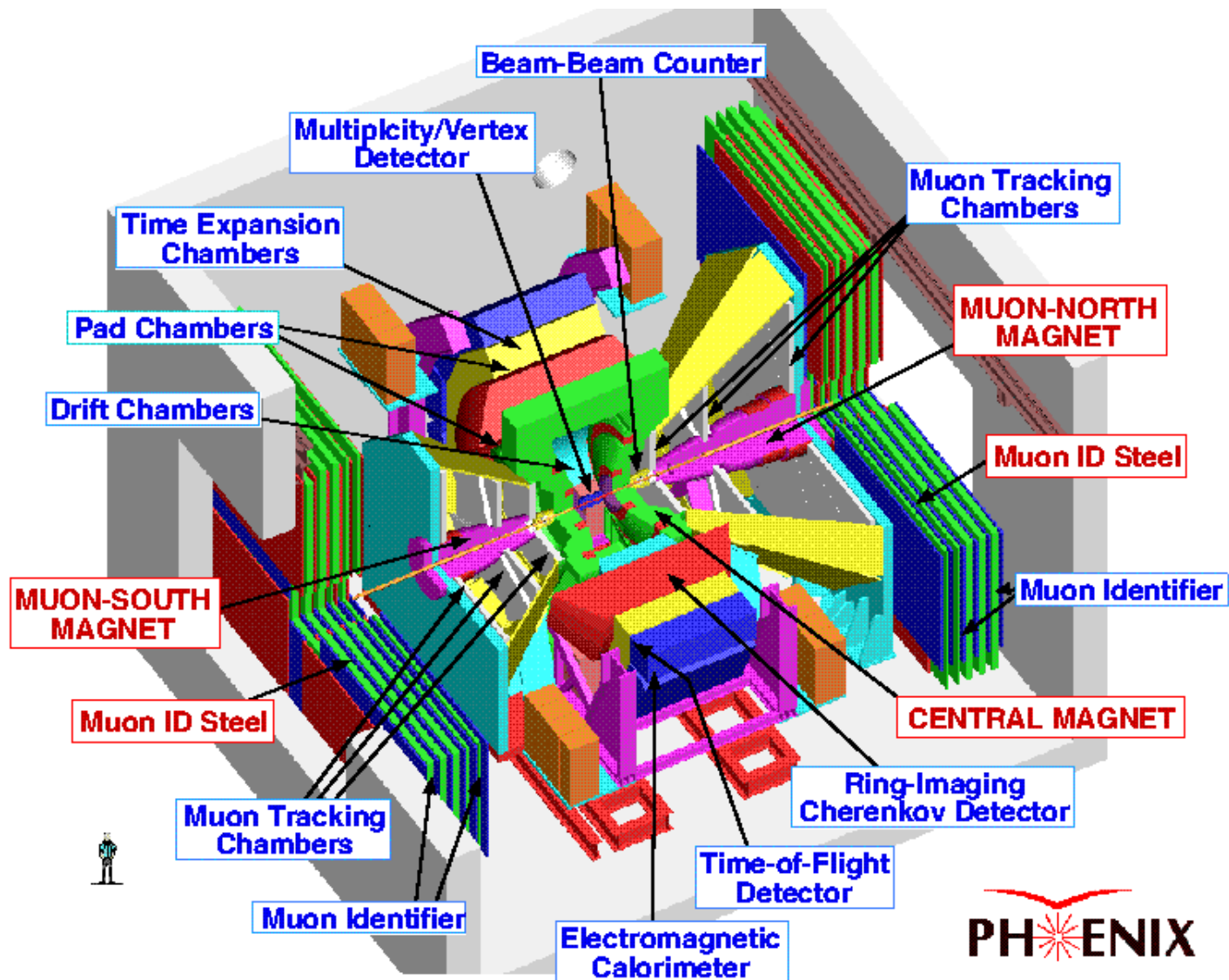


Figure 69: PHENIX detector at RHIC, dedicated to heavy ion collision studies



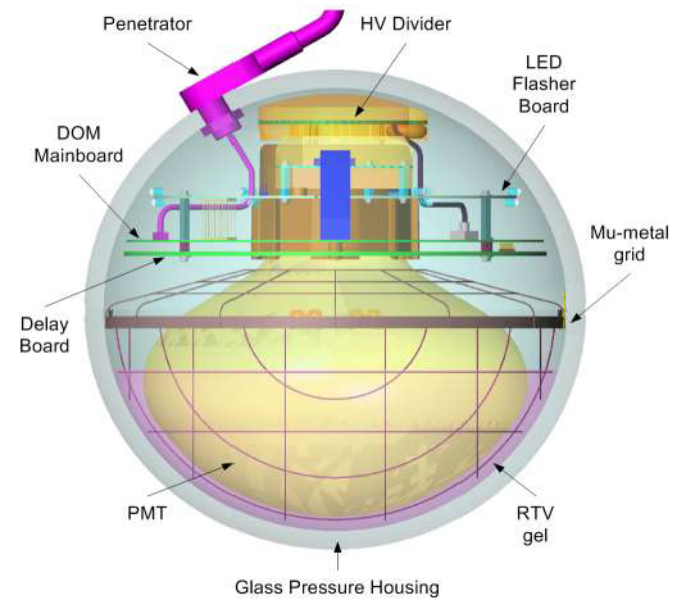
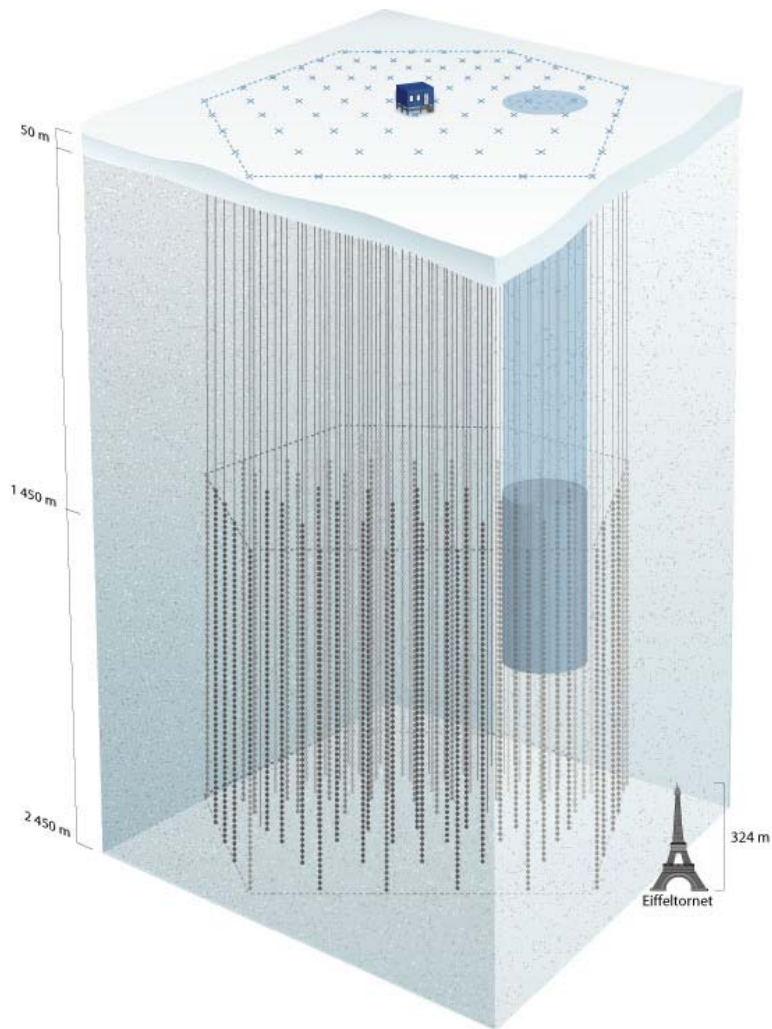


Figure 70: IceCube neutrino detector at the South Pole (left) is an array of photomultiplier modules (right)

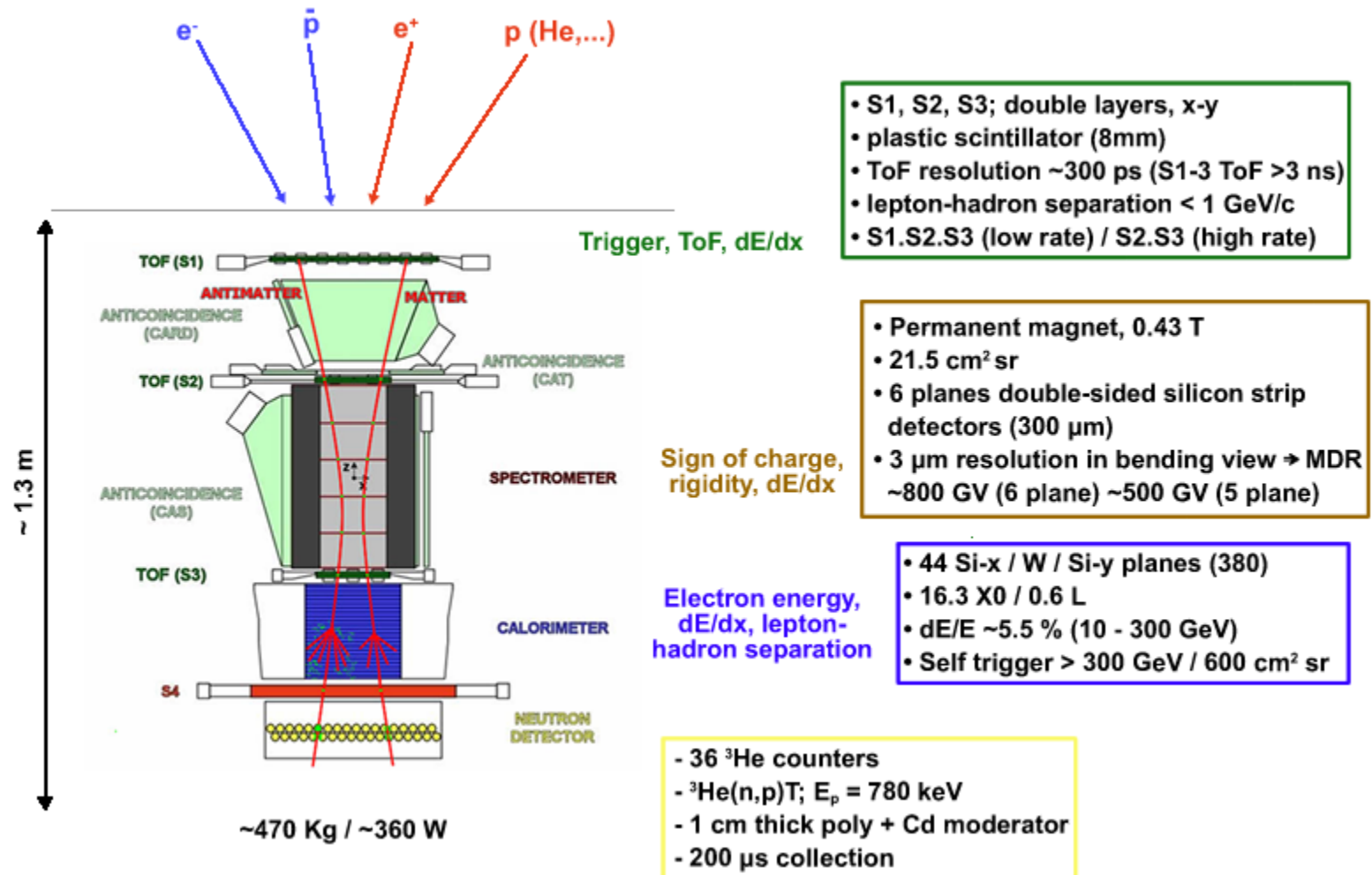


Figure 71: PAMELA detector in space, dedicated to antimatter and astrophysics studies